Reconstruction of 3-D Irregular Shape of Breast Cancer Tumor Using the *Adjoint*-Field Scheme in the Microwave Imaging Algorithm

Magda El-Shenawee[1], Oliver Dorn[2] and Miguel Moscoso[2]

[1]Department of Electrical Engineering
University of Arkansas, Fayetteville, AR 72701, USA
magda@uark.edu

[2]Modeling, Simulation and Industrial Mathematics Group Universidad (GMSMI)
Universidad Carlos III de Madrid, Madrid, Spain
odorn@math.uc3m.es; moscoso@math.uc3m.es

Abstract: This paper presents an algorithm for microwave imaging of breast cancer tumor using a shape reconstruction approach. The algorithm is based on integrating the *adjoint*-field scheme with the method of moments (MoM). The numerical results show good reconstructions of tumors of spherical and non-spherical shapes. We show that employing multiple frequencies, multiple sources and receivers, and multiple polarizations improves the convergence of the algorithm.

Keywords: microwave imaging, breast cancer detection, inverse scattering

1. Introduction

Microwave imaging is showing great promise for the application of early detection of small tumors in the breast. A second challenge associate with the use of microwaves for breast imaging is the discrimination between malignant and benign tumors. Penetration depth of microwaves in human tissue has been reported in the literature to show values in breast carcinoma closer to values in high water content tissue such as muscle, skin and internal organs than to values found in low water content tissue such as fat which predominates in healthy breast [1]. As observed by Hagness *et al* in [2], scattering responses of benign and malignant tumors could be similar since some benign tumors may also have high water content [3]. Therefore, additional criteria for distinguishing between benign and malignant tumors are required.

Benign and malignant tumors could differ significantly in shape. An adenoma (a benign glandular tumor) has a more regular (for example close to spherical) shape while an adenocarcenoma (a malignant glandular tumor) has a more irregular shape [4]. Correctly estimating the shape of a tumor might therefore give additional information about its nature. In a recent study on breast cancer imaging using the Diffuse Optical Tomography (DOT), Boverman *et al* indicated the effect of careful modeling of the breast shape on the ability of accurate imaging [5].

Reconstruction algorithms for microwave data become computationally intensive when searching for three-dimensional (3-D) estimates of the tumor shape [6]. Our recent work has shown a potential of integrating the adjoint-fields scheme with the method of moments (MoM) to reduce the cost for reconstructing the shape of spherical tumors [7]. It is important to emphasize that the work in [6] is a parameter-based shape/location reconstruction algorithm in which the spherical harmonics functions were used to model malignant tumors. In the current paper we present an algorithm which is not based on a parameter-estimation method but uses a surface discretization instead. The goal of this paper is to show the potential of using this adjoint-fields/MoM algorithm in reconstructing breast tumor of irregular shapes with this surface discretization model. We show that a smoothing scheme and a frequency hopping strategy are necessary in order to stabilize the algorithm.

2. Methodology

A. Forward model for our numerical experiments

Even though the reconstruction algorithm employed here is based on a surface discretization, we use a spherical harmonics representation of surfaces for creating simulated data describing the true tumor. Here we follow the work described in [6]. In this representation, the radius at each node on the tumor surface is presented as a function of θ and ϕ angles as:

$$r(\theta,\phi)=\sum_{n=0}^{m}\sum_{m=-n}^{n} a_{nm} Y_n^m(\theta,\phi),\ 0\le\theta\le\pi,\ 0\le\phi\le 2\pi \tag{1a}$$

in which a_{nm} are the harmonic coefficients and the function $Y_n^m(\theta,\phi)$ is the spherical harmonic function given in [6]. Using this representation, the radius $r(\theta,\phi)$ is expressed as (see Appendix B in [6]):

$$\begin{aligned} r(\theta,\phi) = r_0\{&1+r_1\cos(\theta)+r_2\sin(\theta)\cos(\phi)+r_3\sin^2(\theta)\cos(2\phi)+ \\ &r_4\sin(\theta)\cos(\theta)\cos(\phi)+\cdots\} \end{aligned} \tag{1b}$$

The values $r_0, r_1, r_2, \cdots$ represent the spherical harmonic coefficients that can be randomly generated to produce a 3-D irregular shape of the tumor. Notice that the main radius r_0 must be greater than zero. Also, the tumor becomes exactly a sphere of radius r_0 when all other coefficients are zero (i.e. $r_i = 0$ for $i = 1, 2, 3, \ldots$). The expressions in Eq. (1) are used to generate an irregular synthetic tumor to test the surface-discretization based inversion algorithm. The MoM forward solver is used to calculate the electric and magnetic surface current densities on the tumor surface based on the surface discretization into triangular patches [6]. These currents are used to calculate the synthetically measured electric fields at all receivers (synthetic data). The MoM is also used to calculate the scattered electric fields on the tumor surface, $\overline{E}_s$ and $\overline{E}_a$, to be explained in the following section. These values are used to calculate the steepest descent gradient direction in each step of the iterative inversion algorithm.

B. Reconstruction algorithm

The main idea of using the adjoint-fields scheme is to avoid solving the forward solver several times [6]. In fact, using adjoint fields allows us to calculate gradient directions by solving the scattering problem only twice; one for the forward solution and one for the adjoint solution. The mathematical details of the algorithm are provided in [7]. In the current paper, the focus will be on the implementation details. The inversion algorithm can be summarized as follows:

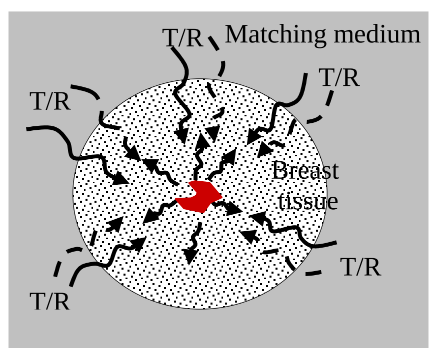

Fig. 1 Breast cross section to show the configuration of the forward and *adjoint*-fields.

1. Choose initial guess of the tumor. In our case this will be a large sphere.
2. Calculate the incident waves at the surface of tumor ($\overline{E}_i$) and employ the MoM for calculating the forward solution (first forward problem) [6]. In particular, calculate the scattered waves at the surface of the tumor ($\overline{E}_s$) and the scattered waves at each receiver for multiple frequencies and polarizations.
3. Calculate the residual error (the mismatch) between these simulated scattered fields and the synthetic measurements at all receivers for all frequencies and polarizations.

4. Use the complex conjugate residuals at all receivers as new sources (new incident waves) and back-propagate the waves to the target. This amounts to solving the adjoint problem (due to reciprocity, this is just a second forward problem) using the MoM. In particular, calculate the back-propagated (adjoint) fields at the surface of the tumor ($\overline{E}_a$) in this case.
5. Combining these solutions of the forward and the adjoint problem at the currently estimated tumor surface, calculate the descent direction c in the normal direction of this surface as $c = \mathrm{Re}\left(\left(\overline{E}_i + \overline{E}_S\right) \cdot \overline{E}_a \left(\hat{\varepsilon}_T^2 - \hat{\varepsilon}_B^2\right)\right)$, where $\hat{\varepsilon}_T$ is the complex relative permittivity of the tumor and $\hat{\varepsilon}_B$ is the complex relative permittivity of the breast background. This gives us an update direction for correcting the surface in a descent direction of the least-squares cost functional.
6. Apply this update at each surface node using: $\overline{x}_{new} = \overline{x}_{old} - \gamma\, c$, where γ is the small step size and $\overline{x}$ represents the coordinates (x, y, z) of each surface node of the tumor.
7. Check the convergence of the algorithm by plotting the cost functional (mismatch) versus the iteration number. Stop the algorithm if a predefined stopping criterion is satisfied (e.g. a low value or a minimum of the cost). Otherwise, continue with step 2. of the algorithm using this latest update as new initial guess.

A cross section of the true 3-D breast and tumor is shown in Fig. 1. The configuration shows the incident waves from the transmitter *T* (solid arrows), the scattered waves from the tumor (reversed solid arrows) and the back-propagated waves from the receiver *R* to the tumor (dotted-arrows) for one step of the inversion algorithm.

3. Numerical Results

A synthetic tumor of irregular shape is generated using Eq(1) where 10 random harmonic coefficients are employed. The computational domain is 20 cm × 20 cm × 20 cm. The relative dielectric constant of the tumor is assumed $\hat{\varepsilon}_T$ =50-*j*12 and the relative dielectric constant of the background is assumed $\hat{\varepsilon}_B$ = 9-*j*1.2. A perfect matching medium is surrounding the breast with the same dielectric constant of the breast background (see Fig. 1). The total number of transmitter/receiver (*T*/*R*) is 40 where 5 *T*/*R* are located at each plane of constant elevation angle (θ = 0.1π to θ = 0.9π), and 8 *T*/*R* at each plane of constant azimuth angle (φ = 0 to φ = 2π). The initial guess of the irregular tumor is assumed a large sphere centered at the same location of the synthetic true tumor.

For simplicity, plane waves are used in this work to excite the synthetic tumor with incident polarization in the θ-direction. The results are for received waves with co-, cross-, or both polarizations. The number of surface nodes of the tumor are 8 and 16, in the θ- and φ-directions, respectively. The step size γ is automatically calculated such that the average displacement of all surface nodes in a given iteration is ~0.5mm.

The focus of this work is to test the surface-based inversion algorithm by updating the location of each surface node according to the calculated gradient. The preliminary results indicate the need of a regularization scheme to stabilize the updates of surface nodes. A simplified method is used in this work as follows:

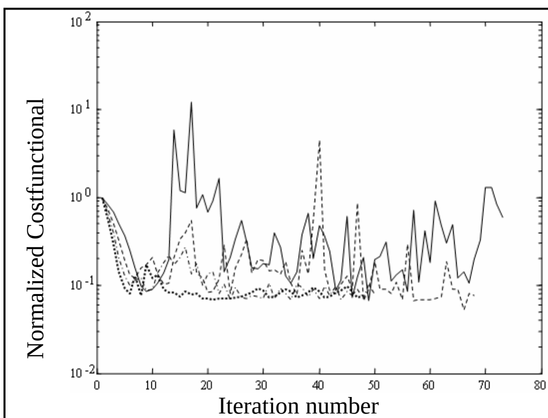

Fig.2 The cost functional vs iteration number for several smoothing values

$$\overline{x}(i)_{new} = \overline{x}(i)_{new} - \alpha \sum_{j=i+1}^{i+N} \overline{x}(j)_{new} / N \tag{2}$$

Here $\overline{x}(i)_{new}$ represents the i^{th} updated node on the surface, α is a smoothing factor ranging from 0 to 1, and N is the total number of selected neighboring nodes surrounding the i^{th} node. In this work, all nodes sharing the neighboring triangular surface patches are used in Eq. (2). Upon applying the above smoothing scheme for a single frequency, the evolution of the cost functional when using α = 4% (solid-line), 8% (dashed-line), 12% (dashed-dot-line) and 16% (dotted-line) are plotted in Fig. 2. The results show some instability in the algorithm occurring after a few iterations (>10) even for α = 16%. These results are observed in several cases, not presented here, regardless of frequency, shape, and polarization. Our numerical experiments have shown that this instability can be reduced or avoided completely by using a frequency hopping scheme where eight frequencies are used in two groups. The first group includes f = 0.7, 0.9, 1.1, …, and 1.7GHz and the second group includes f =3 and 5GHz. A smoothing factor α = 4% is used in this case. The results of Fig. 3a show the evolution of the cost functional versus the iteration number where the first group of frequencies was used up to the 38th iteration, then the higher frequencies are used in the rest of iterations. Fig. 3b-d shows the true tumor (black color) and the reconstructed tumor (grey color) after the 1, 38, and 500 iterations, respectively. The initial guess in this case is a sphere of radius 4cm.

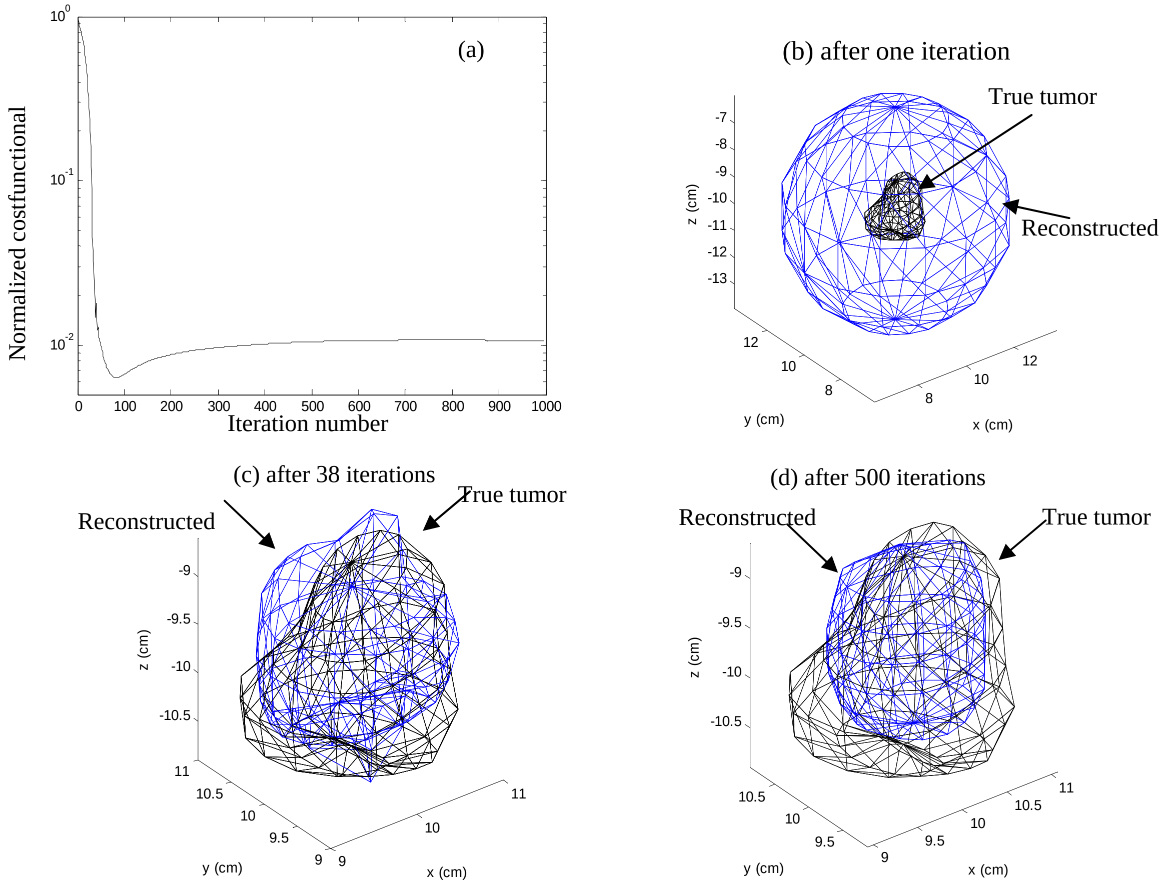

Fig.3 (a) Normalized costfunctional vs iteration number, (b) true and reconstructed tumor after one iteration, (c) after 38 iterations, and (d) after 500 iterations. The smoothing factor α =4%. No noise. Eight frequencies.

A second example is shown in Fig. 4 where twelve frequencies are used in a frequency hopping manner. The first six frequencies are the same as in previous example, while the second group includes f = 3., 3.4, 3.8, …, and 5 GHz. Fig. 4b-d show the reconstructions after 1, 38, and 255 iterations. No noise was added to the data of Figs. 3 and 4.

In order to make the numerical experiments more realistic, random Gaussian noise with standard deviation equal to 0.01 is added to the synthetic data [6]. The convergence is shown in Fig.5a. The reconstructed tumor is plotted after 1, 9, and 255 iterations as shown in Fig. 5b-d. In figures 3-5, the synthetic data include the co- and cross- polarizations.

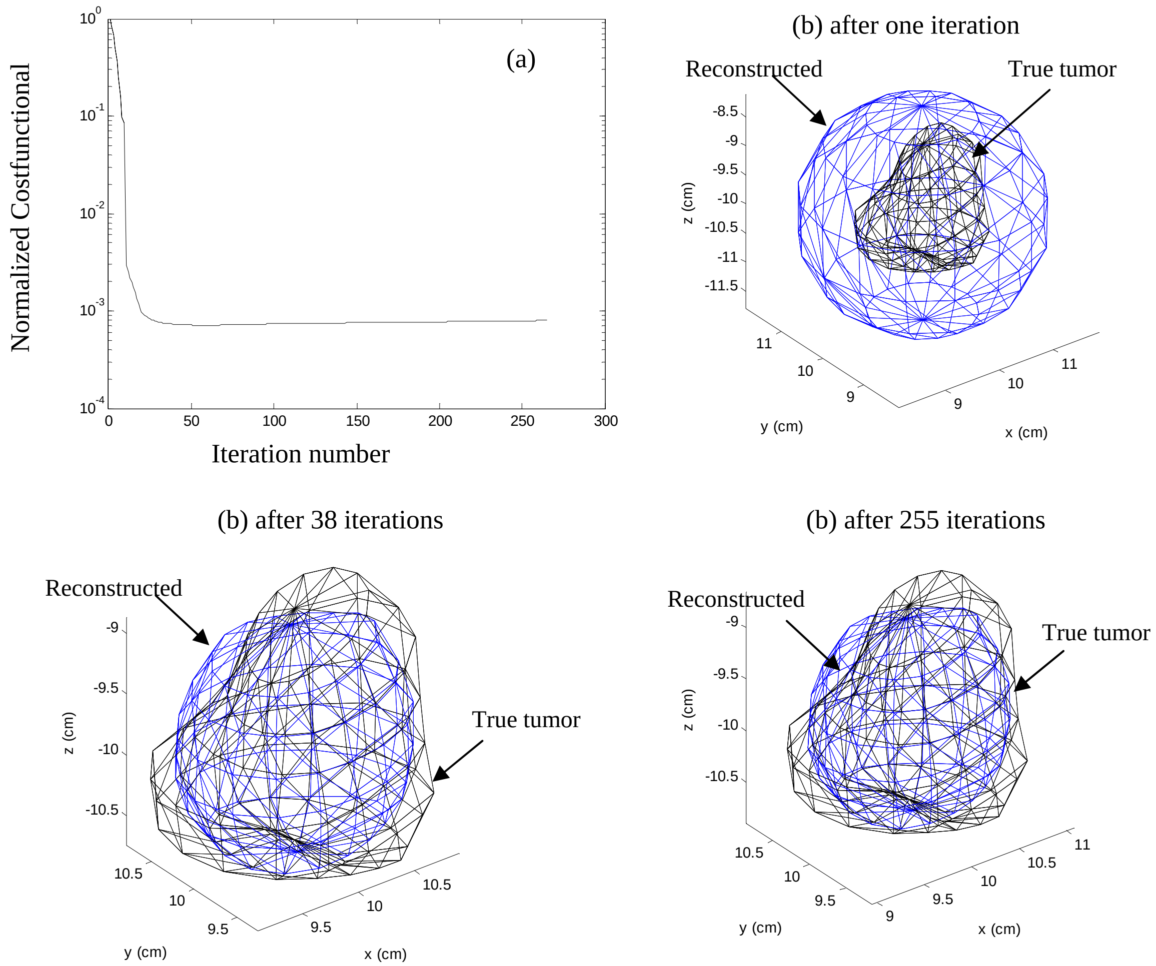

Fig.4 (a) Normalized cost functional vs iteration number, (b) true and reconstructed tumor after one iteration, (c) after 38 iterations, and (d) after 255 iterations. The smoothing factor α =4%. No noise. Twelve frequencies are used.

Conclusion

The results presented in this work show the potential of using the adjoint-field/MoM inversion algorithm for reconstructing irregular shape of breast tumor. The algorithm is surface-based and not parameter- or pixel- based. The use of a smoothing scheme and a frequency hopping technique helped in stabilizing the algorithm.

5. Acknowledgements

This research was sponsored in part by the National Science Foundation award no. ECS-0524042, in part by the Spanish Ministerio de Educación y Ciencia (MEC), Grant nº FIS2004-03767, and in part by the Women Giving Circle at the University of Arkansas grant no. WGC-22.

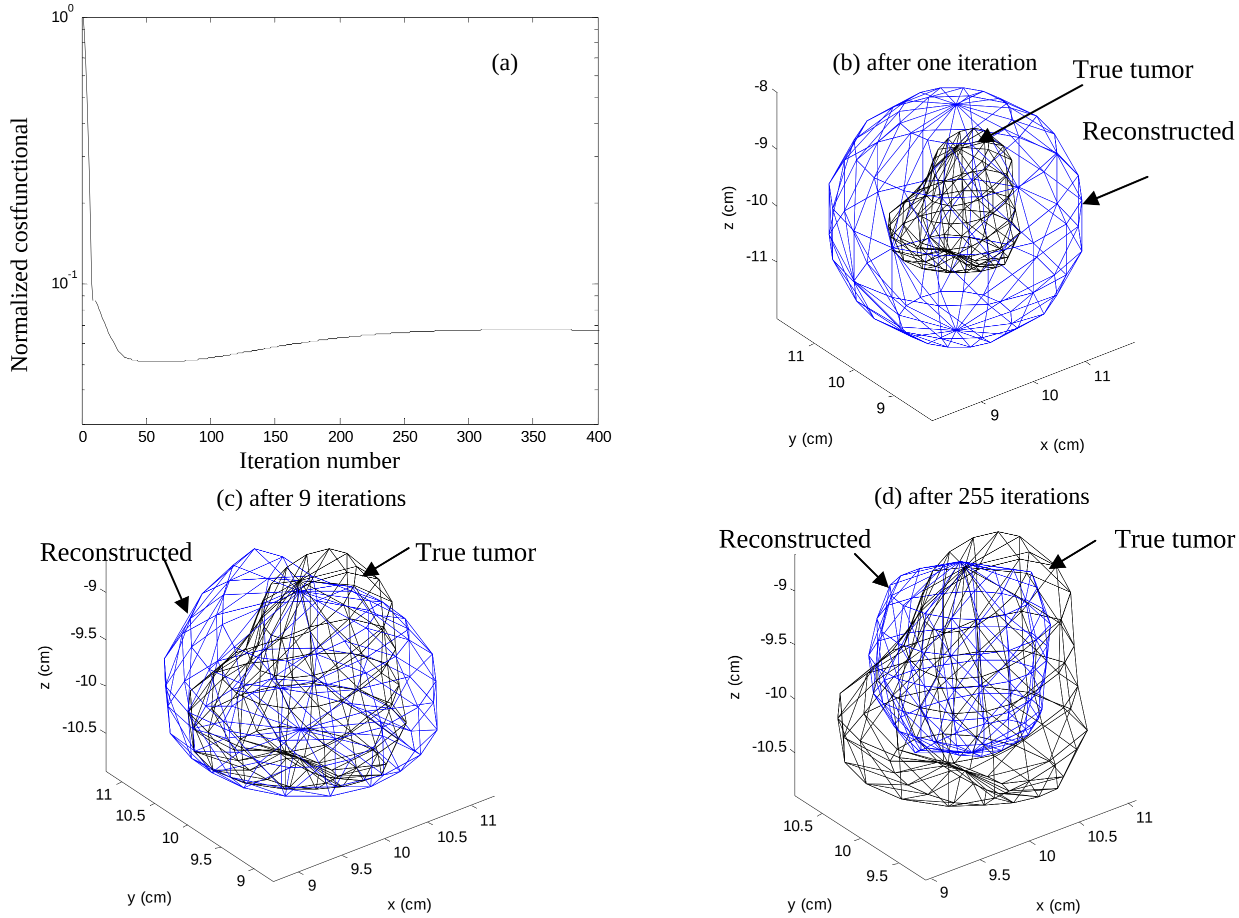

Fig.5 (a) Normalized cost functional vs iteration number, (b) true and reconstructed tumor after one iteration, (c) 9 iterations, and (d) 255 iterations. The smoothing factor α =4%. Added Gaussian noise with standard deviation 0.01. Eight frequencies.

References

[1] Alan H. Barrett and Philip C. Myers, "Basic principles and applications of microwave thermography," in *Medical Applications of Microwave Imaging*, L. E. Larsen and J. H. Jacobi (eds), PP. 41-46, IEEE Press, 1986.

[2] S. Hagness, A. Taflove and J. E. Bridges, "Three-dimensional FDTD analysis of a pulsed microwave confocal systems for breast cancer detection: Design of an antenna-array element," *IEEE Trans. Antennas Propagat.*., vol. 47, pp. 783-791, May 1999.

[3] A. M. Campbell and D. V. Land, "Dielectric properties of female human breast tissue measures *in vitro* at 3.2 GHz," *Phys. Med. Biol.*, vol. 37, no. 1, pp. 193-210, 1992.

[4] Bruce Alberts, Dennis Bray, Julian Lewis, Martin raff, Keith Roberts and James D. Watson, *Molecular Biology of the Cell*, Garland Publishing, Inc. New York & London, second edition, 1989

[5] Gregory Boverman, Ang Li, Quan Zhang, Tina Chaves, Eric L. Miller, Dana H Brooks, and David A Boas, "Quantitative Spectroscopic Diffuse Optical Tomography Guided by Imperfect A Priori Structural Information," *Phys .Med. Biol.*, vol. 50, no. 17, pp. 3941-3956, Sep 2005.

[6] Magda El-Shenawee and Eric Miller, "Spherical Harmonics Microwave Algorithm for Shape and Location Reconstruction of Breast Cancer Tumor," *IEEE Trans. on Medical Imaging*, vol. 25, no. 10, pp. 1258-1271, October 2006.

[7] Oliver Dorn, Magda El-Shenawee, and Miguel Moscoso, "Iterative microwave inversion algorithm based on the adjoint-field method for breast cancer," *Proc. of the 14th European Conference on Mathematics for Industry*, July 10-14, 2006.